Electronic Supplementary Material (ESI) for Reaction Chemistry & Engineering.

Electronic Supplementary Information

An oscillatory plug flow photoreactor facilitates semi-heterogeneous dual nickel/carbon nitride photocatalytic C-N couplings

Cristian Rosso,[a] Sebastian Gisbertz,[b,c] Jason D. Williams,[a,d] Hannes P. L. Gemoets,[e] Wouter Debrouwer,[f] Bartholomäus Pieber*[b] and C. Oliver Kappe*[a,d]

[a] *Institute of Chemistry, University of Graz, NAWI Graz, Heinrichstrasse 28, 8010 Graz, Austria*
[b] *Department of Biomolecular Systems, Max-Planck-Institute of Colloids and Interfaces, Am Mühlenberg 1, 14476 Potsdam, Germany*
[c] *Department of Chemistry and Biochemistry, Freie Universität Berlin, Arnimallee 22, 14195 Berlin, Germany*
[d] *Center for Continuous Flow Synthesis and Processing (CCFLOW), Research Center Pharmaceutical Engineering GmbH (RCPE), Inffeldgasse 13, 8010 Graz, Austria*
[e] *Creaflow BVBA, Industrielaan 12, 9800 Deinze, Belgium*
[f] *Ecosynth NV, Industrielaan 12,-9800 Deinze, Belgium*

*E-mail:

Bartholomaeus.Pieber@mpikg.mpg.de

oliver.kappe@uni-graz.at

Contents

A. General experimental information

A1. Materials and methods

Commercial reagents and solvents were purchased (Sigma-Aldrich, Fluka, Alfa Aesar, Fluorochem or VWR) and used as received, without further purification, unless otherwise stated.
Ethyl 4-bromobenzoate (**1**), pyrrolidine (**2a**), butylamine (**2b**), nickel(II) bromide trihydrate, and 4-ethylbiphenyl were all commercially available. Carbon nitride photocatalyst, CN-OA-m, was synthesized according to the literature procedure.[S1]

Chromatographic purification of products was accomplished using a Biotage Isolera automated flash chromatography system with cartridges packed with KP-SIL, 60 Å (32–63 µm particle size).
For thin layer chromatography (TLC) analysis, Merck pre-coated TLC plates (silica gel 60 GF254, 0.25 mm) were employed, using UV light as the visualizing agent (254 nm), basic aqueous potassium permanganate ($KMnO_4$) stain solution or iodine and heat as developing agents.
Organic solutions were concentrated under reduced pressure on a Büchi rotatory evaporator.

NMR spectra were recorded on Bruker 300 MHz spectrometer (^{1}H: 300 MHz, ^{13}C: 75 MHz, ^{19}F: 282 MHz). The chemical shifts (δ) for ^{1}H, ^{13}C and ^{19}F are given in ppm relative to residual signals of the solvent ($CDCl_3$ at 7.26 ppm ^{1}H-NMR and 77.16 ppm ^{13}C-NMR). Coupling constants are given in Hertz (Hz). The following abbreviations are used to indicate the multiplicity: s, singlet; d, doublet; t, triplet; q, quartet; dd, doublet of doublets; ddd, doublet of doublet of doublets; m, multiplet.

Analytical HPLC (Shimadzu LC20) analysis were carried out on a C18 reversed-phase (RP) analytical column (150 mm × 4.6 mm, particle size 5 µm) at 37 °C using mobile phases A (90:10 v/v water/acetonitrile + 0.1% TFA) and B (MeCN +0.1% TFA) at a flow rate of 1.5 mL/min. The following gradient was applied: linear increase from 30% to 100% B over 10 min.

UV-Vis spectra were recorded using a fiber-coupled Avantes Starline AvaSpec-2048 spectrometer, with an Avantes AvaLight-DHc lamp as the light source. These spectra were processed using Avasoft 8.7 software.

Centrifugation was performed using an Eppendorf Centrifuge 5804.

Laser diffraction (LD) analyses were carried out on a Sympatec Helos H2395 particle sizing instrument. Approximately 1 mg of solid was added to 50 mL of deionized water in a cuvette, followed by a small drop of tween 80 surfactant (to aid suspension). The sample in the cuvette was then sonicated for approximately 5 s, and was stirred at 1000 rpm during measurements. Two separate 30 s measurements were taken, to cover a combined particle size range of 0.45-875 µm.

A2. Photoreactor setup

All photochemical reactions were conducted in a commercial continuous-flow reactor: Creaflow HANU$^{\text{TM}}$ Reactor (Fig. S1).

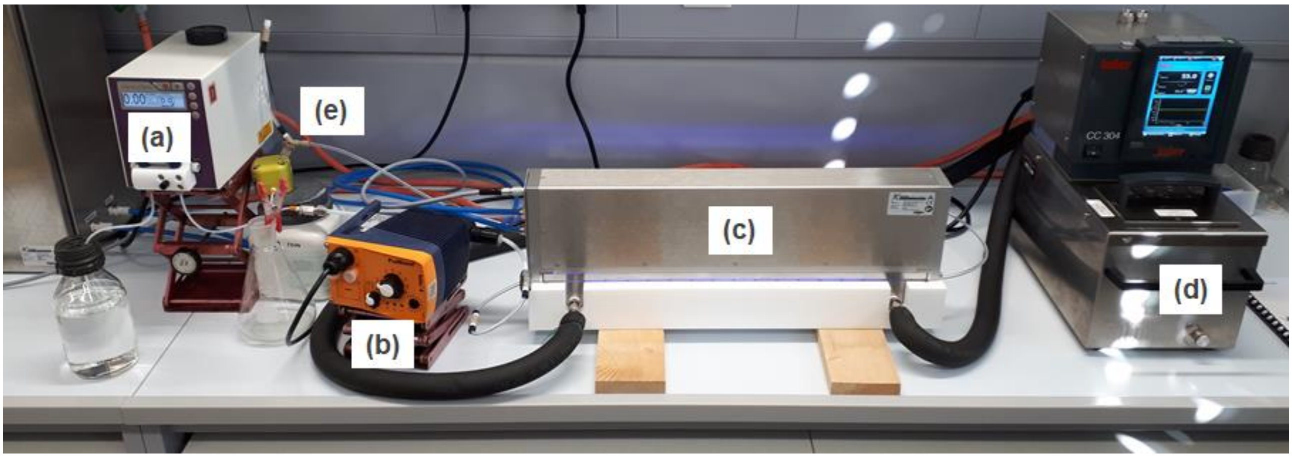

Fig. S1. Photograph of commercial photoreactor setup: a) metering peristaltic pump (SF-10, Vapourtec); b) pulsator (Creaflow customized ProMinent (beta/4) pump with PTFE/carbon pump head); c) Reactor Module consisting of a HANU$^{\text{TM}}$ reactor and Peschl LED module; d) temperature control for reaction plate (Huber); e) backpressure regulator (BPR-10, Zaiput) with Creaflow pulsation dampener. Photograph of the LED control panel, containing the cooling system, has been omitted.

Reactor module (HANU$^{\text{TM}}$ HX 15-C276-CUB reactor, Creaflow): A Hastelloy-based microstructured plug flow reactor (540 × 60 × 60 mm size; channel dimensions: 480 × 20 × 2 mm, 15 mL internal volume) held in a PTFE housing.

Light source: LED module ("novaLIGHT FLED75" water cooled high-performance LED array, Peschl Ultraviolet) was mounted on the top of the reactor plate (35 mm from the center of the reaction channel). The LED panel (460 nm) was equipped with 36 LEDs (3 strips of 12 LEDs).

Table S1. Power and radiation flow of LEDs used in this study.

Wavelength (nm)	Maximum Current (mA)	Radiation Flow at Maximum Current (W)	Width at 50% intensity (nm)
460	700	33.75[a]	17.5

[a] Radiative flow extrapolated from data (at lower current) provided by the LED manufacturer.

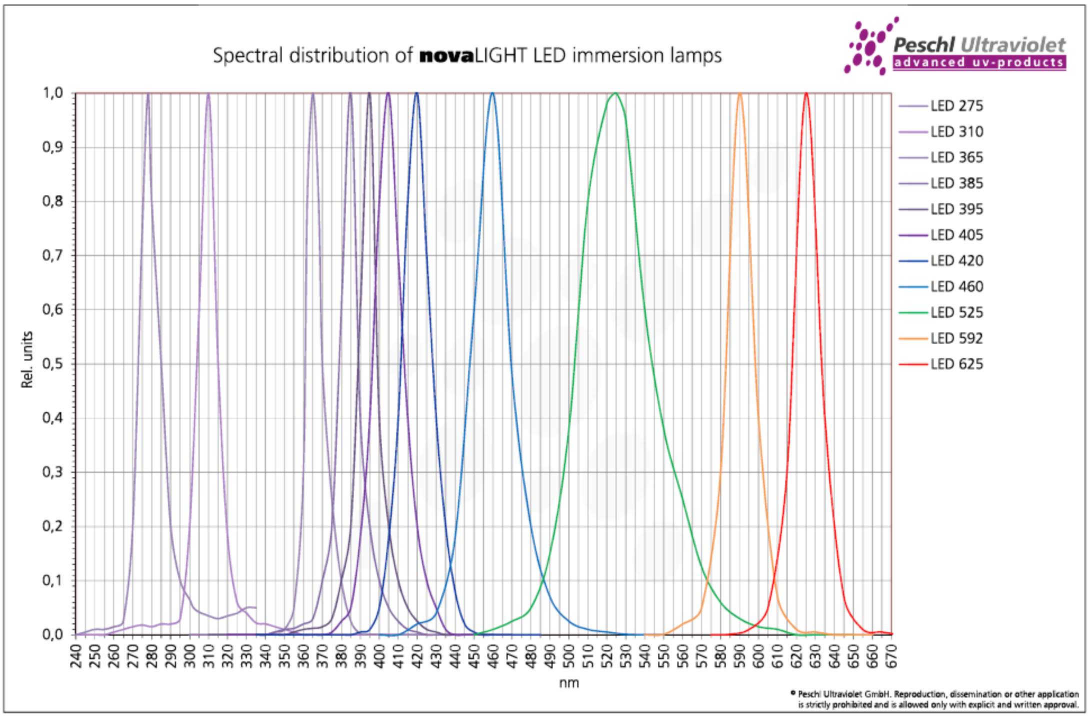

Fig. S2. Emission spectra of LEDs used in this study (460 nm). **Note:** intensities are normalized.

Temperature control: Thermal regulation of the reactor was carried out using a Huber CC304 thermostat filled with silicon oil (temperature range –20 °C to 195 °C).

Metering pump: The feed mixture was conveyed through the reactor using a Vapourtec SF-10 peristaltic pump equipped with “blue” peristaltic tubing (0.02-10.00 mL/min) as metering pump.

Pulsator: Between the metering pump and the reactor, the feed mixture was pulsed using a Creaflow customized ProMinent Beta/4 pump (PTFE/carbon pump head). This had a tunable amplitude (<5-100%), which was experimentally found to constitute a range of approximately 0.04-0.44 mL per stroke (see Fig. S7). The frequency could be tuned from 10-100%, corresponding to a range of 0.3-3 Hz.

Pulsation dampener: The pulsation dampener was constituted by a piece of 1/4” PFA tubing, filled with air, closed on one side and connected in between the reactor output and the backpressure regulator through a PEEK Y-piece.

Back pressure regulator: A dome-type back pressure regulator (Zaiput Flow Technologies, BPR-10) was installed after the pulsation dampener with a set point of 3 bar.

General connections: Connection between the starting mixture flask and the metering pump was achieved using 1/8” o.d. (~1.6 mm i.d.) PTFE tubing with PEEK fittings. Connection between the metering pump and the pulsator was achieved using 1/8” o.d. (~1.6 mm i.d.) PTFE tubing with PEEK fittings and 1/4” o.d (3.2 mm i.d.) PFA tubing with stainless steel (Swagelok) fittings. Reactor plate input and output, as well as pulsation dampener were connected using 1/4” (3.2 mm i.d.) PFA tubing (Swagelok) with PEEK fittings. Backpressure regulator input and output was achieved using 1/8” o.d. (1.6 mm i.d.) PFA tubing with PEEK fittings. Fittings were lined with PTFE tape, to ensure a tight seal.

B. Reactor characterization

B1. Control reactions examining effect of reaction protocol on concentration/yield

The profile of concentration/yield under two different regimes was examined, in order to gain information on the cause of the unexpected trend. To determine whether this was due to difficulty in reaching steady state, a reaction with a "pre-filled" reactor was attempted, and a reaction simply using a larger volume of stock solution (50 mL rather than 25 mL). The results of these reactions are shown below (Fig. S3), whereby a similar trend was still observed, leading to the conclusion that this is not the cause of the unexpected behaviour.

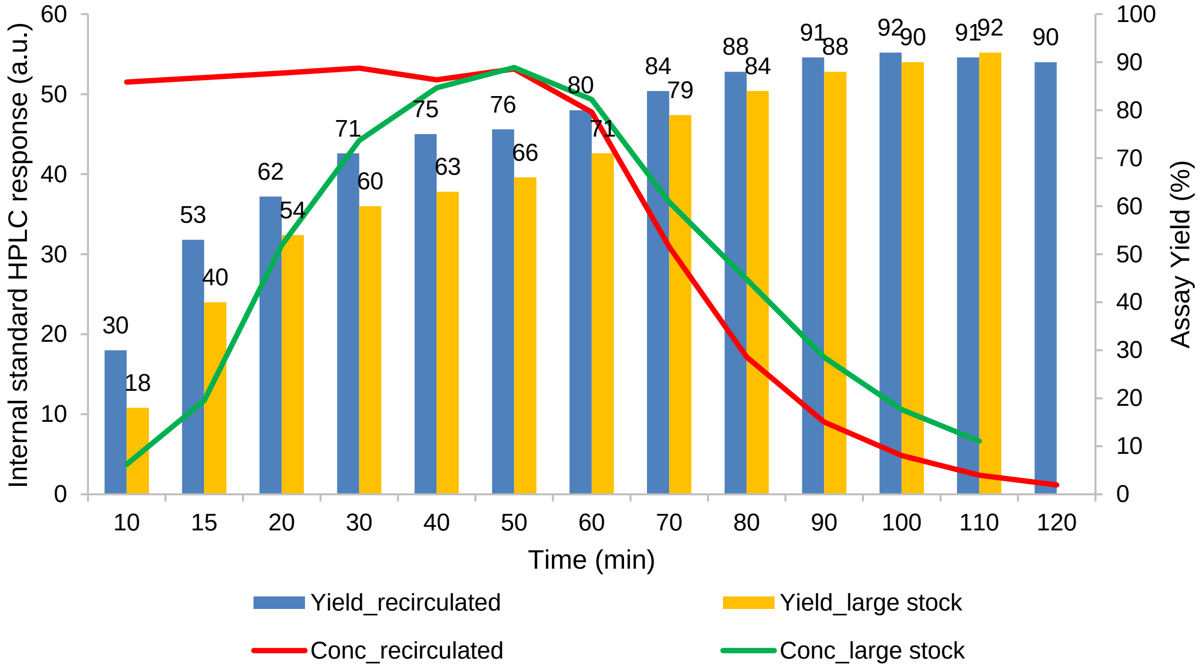

Fig. S3. Two control experiments: a) Rather than starting with a solvent-filled reactor and swapping the pump input to reaction mixture, a 50 mL solution of reaction mixture was circulated through the reactor, to ensure a constant concentration, prior to turning on the LEDs. b) The standard reaction procedure was used, but with a 50 mL solution of reaction material, rather than 25 mL.

B2. Comparison of background reaction between two reactors

In order to determine the cause of the unusual concentration/yield profiles observed (as described in the manuscript), a comparison was carried out, whereby the reaction without carbon nitride photocatalyst (background reaction only) was performed in the HANU^{TM} reactor and Corning Lab Photo Reactor. The resulting trends are shown below (Fig. S4 and Fig. S5). The difference in concentration/yield trends implies that this behaviour is due to the characteristics of the reactor.

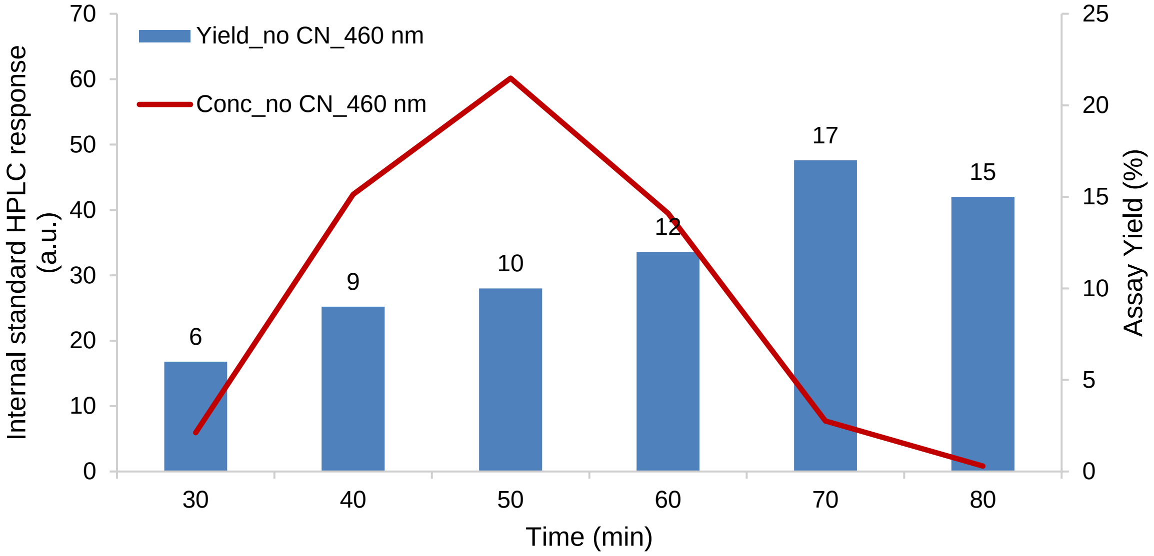

Fig. S4. Results of the background reaction performed in the HANU^{TM} reactor, without carbon nitride photocatalyst. This demonstrates the trend of increasing yield over time, irrespective of concentration.

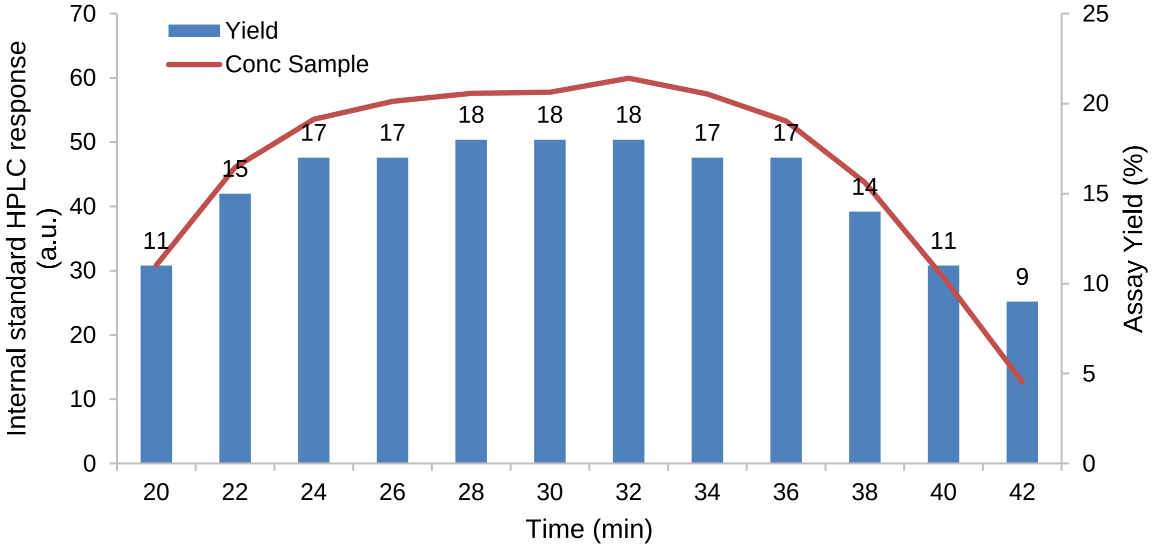

Fig. S5. Results of the background reaction performed in the Corning Lab Photo reactor using 395 nm lamps, without carbon nitride photocatalyst. This demonstrates the expected trend of increasing yield with increasing concentration.

B3. Correlation between pulsation amplitude and displaced volume

An array of experiments was carried out in order to determine the physical correlation between the pulsation amplitude generated by the pulsator and the corresponding displaced volume. For this purpose, a 50 cm length of PFA tubing (1/4” o.d., ~3.2 mm i.d.) was installed after the pulsator and attached to a ruler (see Fig. S6). The system was filled with toluene, then a solution of methylene blue in water was pumped through to provide a liquid/liquid biphasic mixture inside the aforementioned tubing. In absence of any net flow rate, the pulsator was switched on, allowing the colored slugs to move back and forth inside the tube. The overall motion was recorded using a camera set at high frame per seconds rate (240 FPS) giving the possibility to calculate the resulting displaced volume for the selected pulsation amplitude.

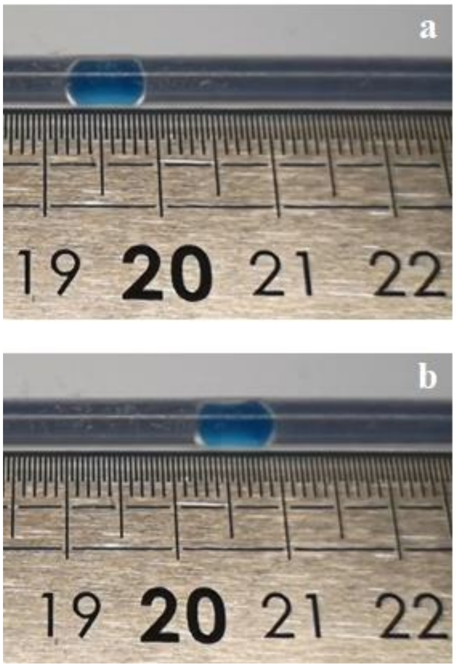

Fig. S6. Tubing installed after the pulsator, attached to a ruler for the displaced volume determination. a) Initial position of the considered tracer slug after the backward pulsation. b) Final position of the considered tracer slug after the forward pulsation.

A linear relationship was observed between the pulsation amplitude and the displaced volume in absence of any net flow rate (Fig. S7).

Pulsation Amplitude	Displaced Volume (mL)
<5%	0.036
10%	0.080
20%	0.120
30%	0.161
50%	0.265
70%	0.297
100%	0.442

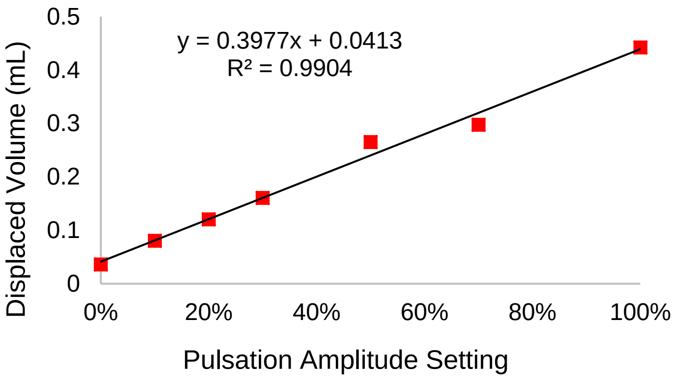

Fig. S7. Correlation between pulsation amplitude and displaced volume.

B4. Residence Time Distribution (RTD) experiments

Residence time distribution (RTD) experiments were performed as shown in Scheme S1. Rose Bengal was used as a tracer in DMAc solution (10^{-4} M concentration) and injected *via* a Y-piece mixer between the metering pump and the pulsator, in a carrier stream of pure DMAc. An in-line UV/Vis flow cell was installed after the back pressure regulator and connected to a spectrometer. Both the reaction setups for the screening experiments (see Fig. S1) and for the scale-out experiment (see Fig. S10) have been characterized in terms of RTD.

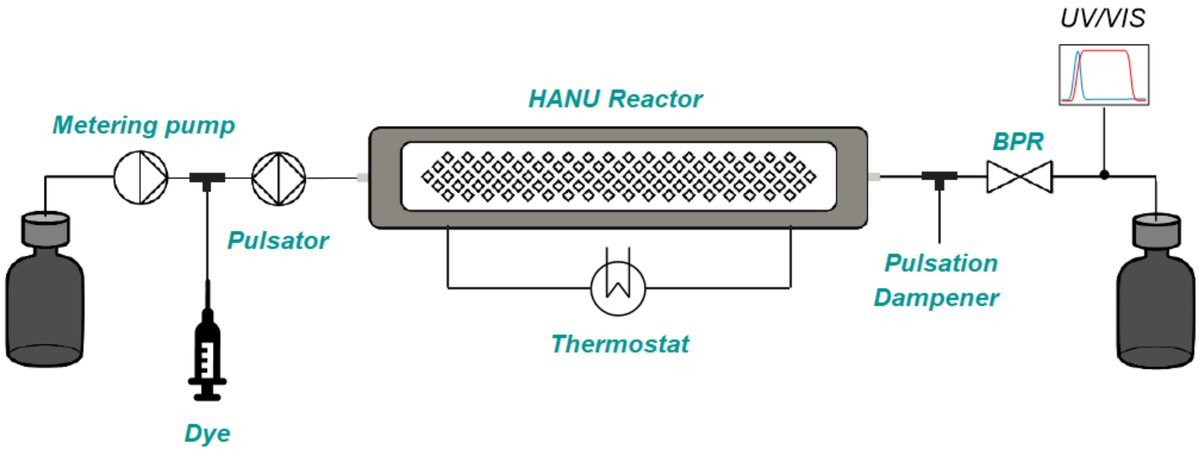

Scheme S1. Flow diagram showing the setup for the RTD experiments.

The RTD profiles for the screening experiments setup are shown in Fig. S8 and the profiles for the scale-out setup are shown in Fig. S9.

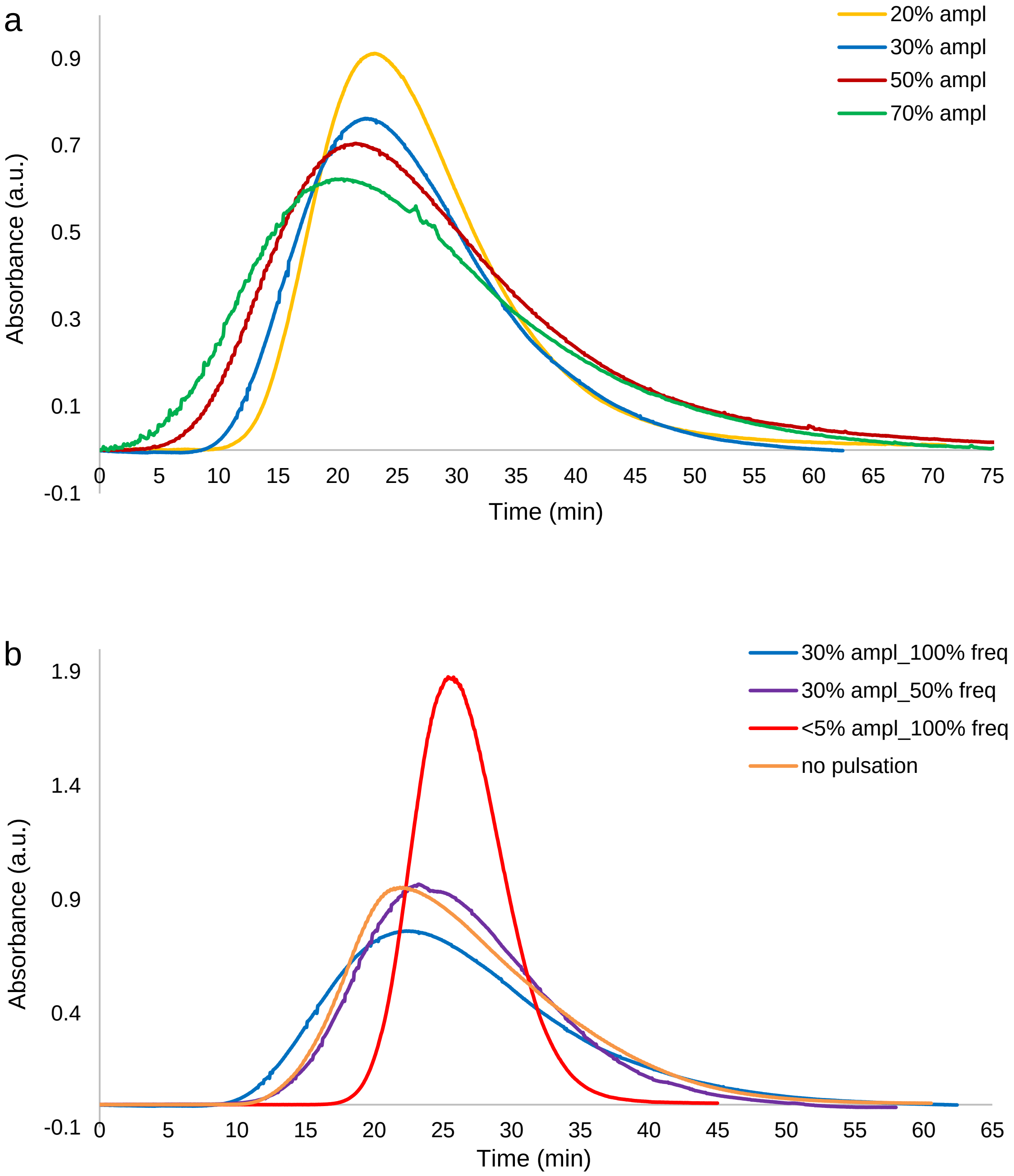

Fig. S8. RTD profiles at 563 nm in DMAc for the screening experiments setup. Conditions: flow rate = 1 mL/min, backpressure = 3 bar, tracer injected volume = 2 mL, optical path length = 1 cm. a) Experiments performed at 100% pulsation frequency and different pulsation amplitudes. b) Experiments performed at different pulsation frequencies.

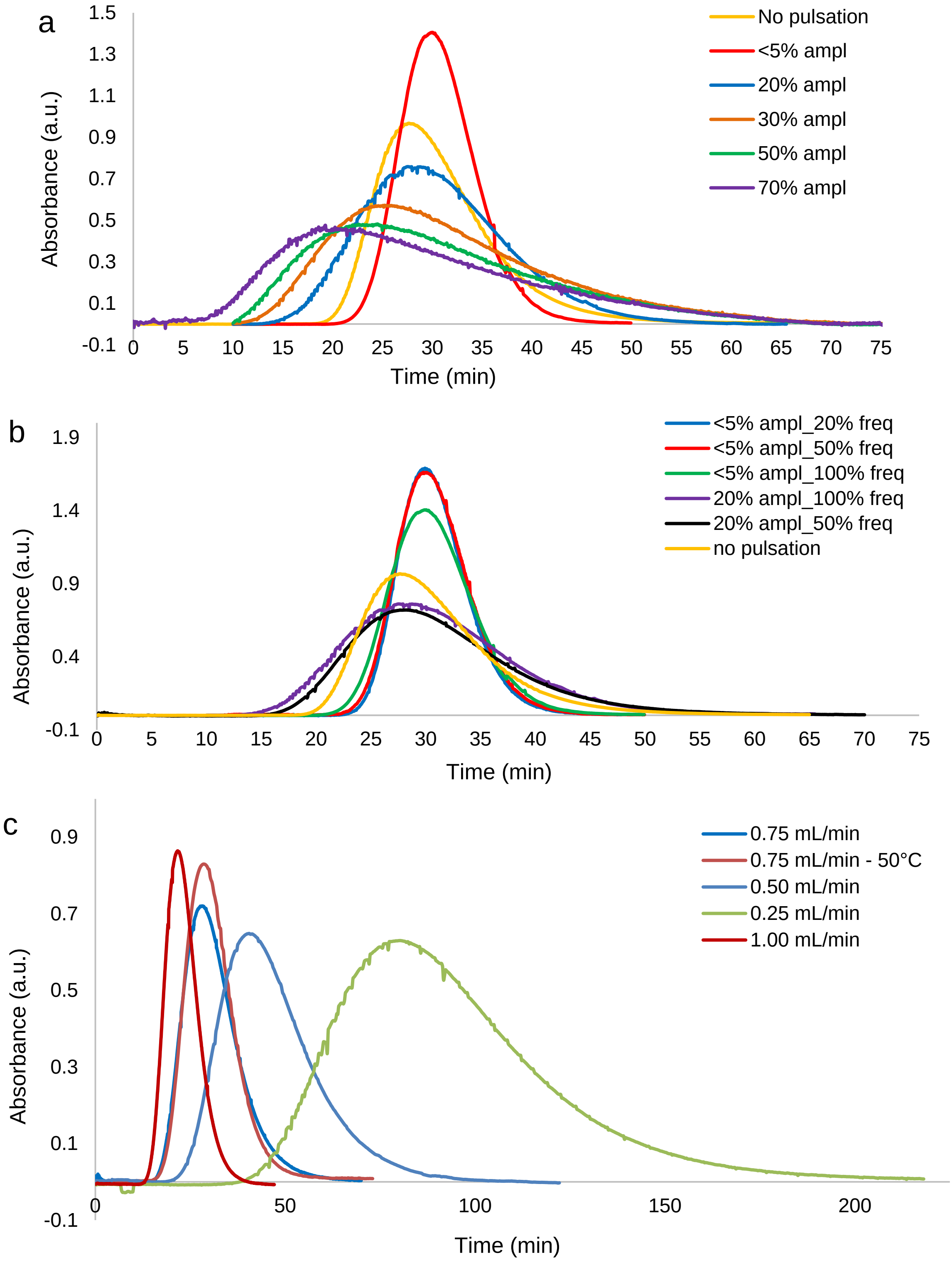

Fig. S9. RTD profiles at 563 nm in DMAc for the scale-out setup. Conditions: flow rate = 0.75 mL/min, backpressure = 3 bar, tracer injected volume = 1 mL, optical path length = 1 cm. a) Experiments performed at 100% pulsation frequency and different pulsation amplitudes. b) Experiments performed at different pulsation frequencies. c) Experiments performed at different flow rates (at 25°C, unless differently stated).

From each of these RTD profiles, the dimensionless Bodenstein (Bo) number was calculated, consisting of the mean residence time ($\bar{t}$) multiplied by two, divided by the variance (σ^2):

$$Bo = \frac{2 \cdot \bar{t}}{\sigma^2}$$

The variance can be calculated from a given RTD experiment using the following formula:

$$\sigma^2 = \frac{\sum t_i^2 \cdot C_i \cdot \Delta t}{\sum C_i \cdot \Delta t} - \bar{t}^2$$

A Bo value greater than 100 indicates that plug flow behavior is exhibited.[S2]

Table S2. RTD experiments in the scale-out setup, performed under different pulsation and flow settings, with their corresponding Bodenstein (Bo) numbers, to characterize the extent of axial dispersion in each case. Higher Bo corresponds to a lesser extent of back mixing.

Entry	Flow rate (mL/min)	Pulsation Amplitude (mL/%)	Pulsation Frequency (Hz/%)	Bodenstein number
1	0.75	0 / 0	0/0	48
2	0.75	0.04 / <5	3 / 100	128
3	0.75	0.12 / 20	3 / 100	35
4	0.75	0.16 / 30	3 / 100	16
5	0.75	0.24 / 50	3 / 100	13
6	0.75	0.32 / 70	3 / 100	10
7	0.75	0.04 / <5	1.5 / 50	153
8	0.75	0.04 / <5	0.6 / 20	184
9	0.75	0.12 / 20	1.5 / 50	32
10	0.25	0.12 / 20	1.5 / 50	23
11	0.5	0.12 / 20	1.5 / 50	25
12	1	0.12 / 20	1.5 / 50	76
13[a]	0.75	0.12 / 20	1.5 / 50	33

C. General procedures

C1. General procedure for the model reaction: screening experiments and scale-out

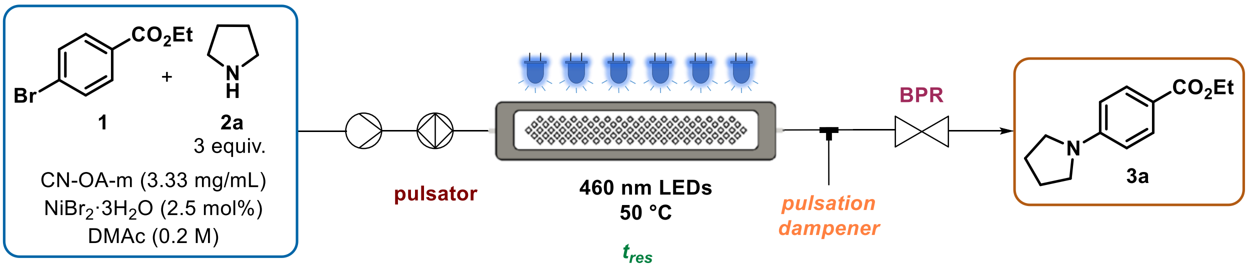

Scheme S2. Flow diagram showing general reaction setup for screening experiments.

The LED array, equipped with 460 nm LEDs, was switched on and the reaction plate thermostat was set to 50 °C. A mixture of ethyl 4-bromobenzoate **1** (5 mmol, 1 equiv), pyrrolidine **2a** (15 mmol, 3 equiv), CN-OA-m (3.33 mg/mL with respect to the solvent, 83.2 mg), nickel(II) bromide trihydrate (0.125 mmol, 2.5 mol%), 4-ethylbiphenyl (internal standard, 0.5 mmol, 0.1 equiv) was made up in *N*,*N*-dimethylacetamide (25 mL total volume in a flask, $[\mathbf{1}]_0 = 0.2$ M). Using the back pressure regulator, a pressure of 3 bar was set. The reaction mixture was degassed prior to use by sparging with an argon balloon for 15 minutes, then pumped through the reactor at 0.75 mL/min flow rate, corresponding to 20 min residence time. The pulsator was set to 20% (0.12 mL) pulsation amplitude and 50% (1.5 Hz) pulsation frequency. Samples were collected over the time for analysis by HPLC, after filtration (0.45 μm syringe filter).

For the scale-out experiment, the setup shown in Fig. S10 was used. A mixture of ethyl 4-bromobenzoate **1** (75 mmol, 1 equiv), pyrrolidine **2a** (225 mmol, 3 equiv), CN-OA-m (3.33 mg/mL, with respect to the solvent, 832 mg), nickel(II) bromide trihydrate (1.88 mmol, 2.5 mol%), 4-ethylbiphenyl (internal standard, 7.5 mmol, 0.1 equiv) was made up in *N*,*N*-dimethylacetamide (250 mL total volume in a flask, $[\mathbf{1}]_0 = 0.3$ M). Using the back pressure regulator, a pressure of 3 bar was set. The reaction mixture was degassed prior to use by sparging with an argon balloon for 30 minutes, then pumped through the reaction plate at 0.75 mL/min flow rate, corresponding to 20 min residence time, 20% (0.12 mL) pulsation amplitude and 50% (1.5 Hz) pulsation frequency. In order to avoid particle settling in the tubing, a vibrating motor (Fig. S11) was installed on the peristaltic pump inlet and a small argon bubble was introduced to the system from the headspace of the starting mixture vessel every 15 minutes. Samples were collected over the time for analysis by HPLC, after filtration (0.45 μm syringe filter). The processed mixture, containing compound **3a**, was collected in the steady state over 270 min (4 hours and 30 min, from minute 50 to minute 320, providing a theoretical yield of 60.75 mmol, see Fig. S12).

The crude reaction mixture was centrifuged at 6000 rpm for 5 minutes and the liquid phase was carefully separated before being diluted with water and extracted with ethyl acetate. The combined organic phases were washed with water, $NaHCO_3$ saturated solution and brine, dried over sodium sulfate and concentrated. The crude product was purified by trituration with petroleum ether and filtration to give the corresponding aryl amino compound **3a**.

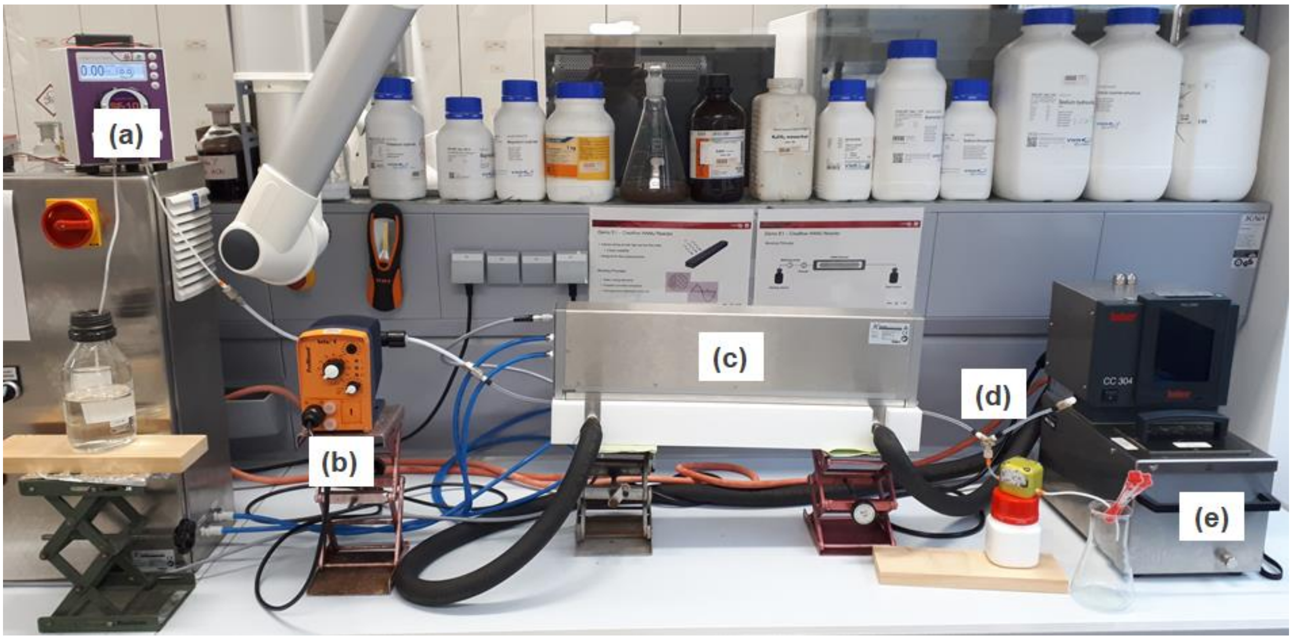

Fig. S10. Photograph of commercial photoreactor setup for the scale-out experiment: a) metering peristaltic pump (Vapourtec); b) pulsator; c) reactor module housing, within the reaction plate and the LED module on the top; d) backpressure regulator with pulsation dampener; e) temperature control for the reactor (Huber).

Fig. S11. Photograph of commercial vibrating motor and the battery power supply installed on the peristaltic pump inlet.[S3]

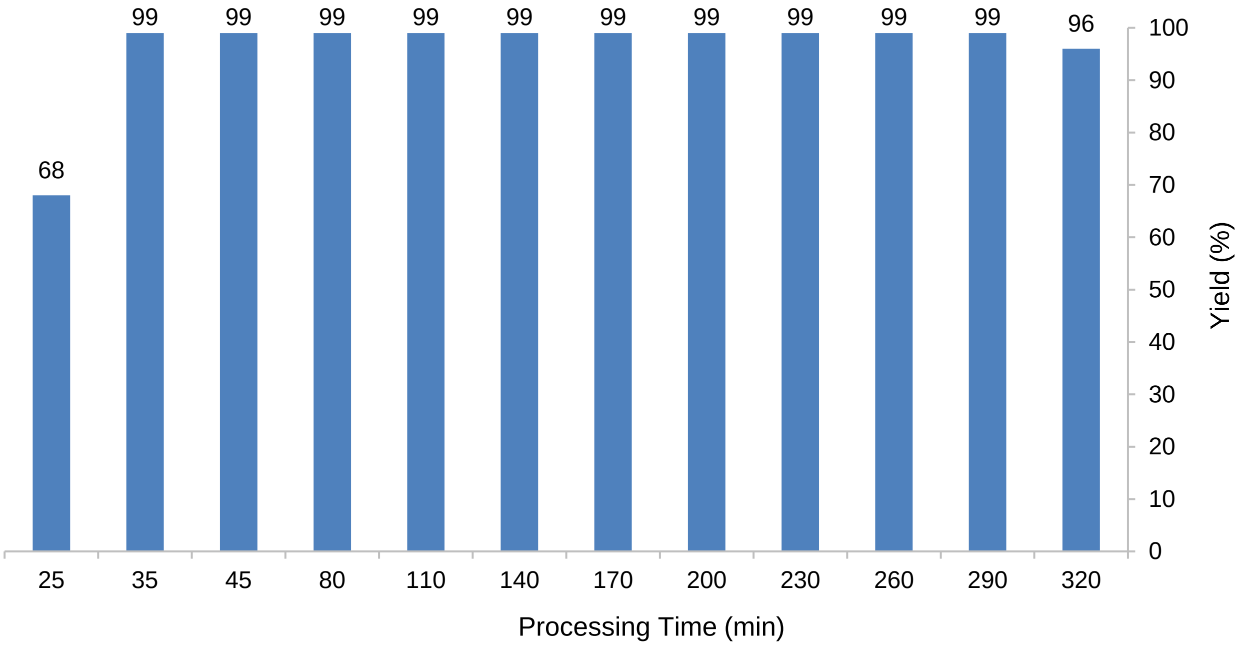

Fig. S12. HPLC yield profile of the model reaction samples collected over the run time.

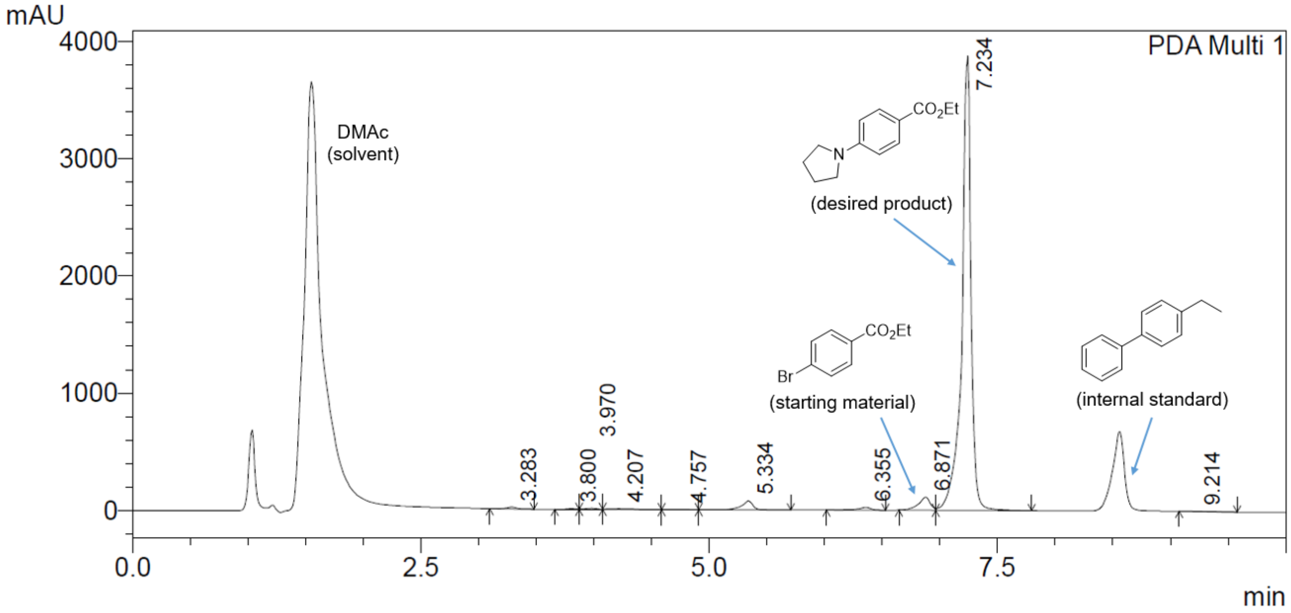

Fig. S13. HPLC chromatogram of the collected long run material, prior to workup.

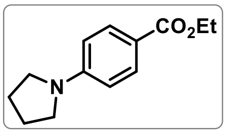

Ethyl 4-(pyrrolidin-1-yl)benzoate (3a). Prepared according to the scale-out procedure **C1**. The product **3** was obtained as an off-white solid (12.05 g, 90% yield). The characterization of the compound matches the data reported in the literature.[S4]

Fig. S14. Photograph of the isolated coupling product **3a**.

C2. General procedure for the tetracaine precursor synthesis: Screening experiments and isolation run

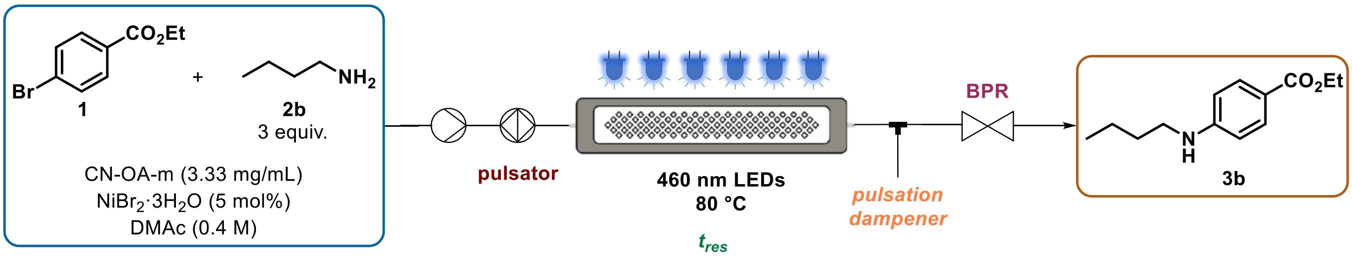

Scheme S3. Flow diagram showing the reaction setup for the tetracaine intermediate **3b** synthesis.

The LED array, equipped with 460 nm LEDs, was switched on and the reaction plate thermostat was set to 80 °C. A mixture of ethyl 4-bromobenzoate **1** (10 mmol, 1 equiv), butylamine **2b** (30 mmol, 3 equiv), CN-OA-m (3.33 mg/mL with respect to the solvent, 83.2 mg), nickel(II) bromide trihydrate (0.5 mmol, 5 mol%), 4-ethylbiphenyl (internal standard, 1 mmol, 0.1 equiv) was made up in *N*,*N*-dimethylacetamide (25 mL total volume in a flask, $[\mathbf{1}]_0$ = 0.4 M). Using the back pressure regulator, a pressure of 3 bar was set. The reaction mixture was degassed prior to use by sparging with an argon balloon for 15 minutes, then pumped through the reactor at 0.25 mL/min flow rate, corresponding to 60 min residence time. Samples were collected over the time for analysis by HPLC, after filtration (0.45 µm syringe filter).

For the isolation run experiment, setup shown in Fig. S10 was used. A mixture of ethyl 4-bromobenzoate **1** (30 mmol, 1 equiv), butylamine **2b** (90 mmol, 3 equiv), CN-OA-m (3.33 mg/mL with respect to the solvent, 250 mg), nickel(II) bromide trihydrate (1.5 mmol, 5 mol%), 4-ethylbiphenyl (internal standard, 3 mmol, 0.1 equiv) was made up in *N*,*N*-dimethylacetamide (75 mL total volume in a flask, $[\mathbf{1}]_0$ = 0.4 M). Using the back pressure regulator, a pressure of 3 bar was set. The reaction mixture was degassed prior to use by sparging with an argon balloon for 30 minutes, then pumped through the reactor at 0.25 mL/min flow rate, corresponding to 60 min residence time. In order to avoid particles settling in the tubing, a vibrating motor (Fig. S11) was installed on the peristaltic pump inlet and a small argon bubble was let enter to the system from the headspace of the starting mixture vessel every 15 minutes. Samples were collected over the time for analysis by HPLC, after filtration (0.45 µm syringe filter). The processed mixture, containing compound **3b**, was collected in the steady state over 80 min (from minute 140 to minute 220, providing a theoretical yield of 8 mmol, see Fig. S15).

The crude mixture was centrifuged at 6000 rpm for 5 minutes and the liquid phase was carefully separated before being evaporated under reduced pressure. The residue was purified by column chromatography (petroleum ether/ethyl acetate 80:20) to give the corresponding tetracaine precursor **3b**.

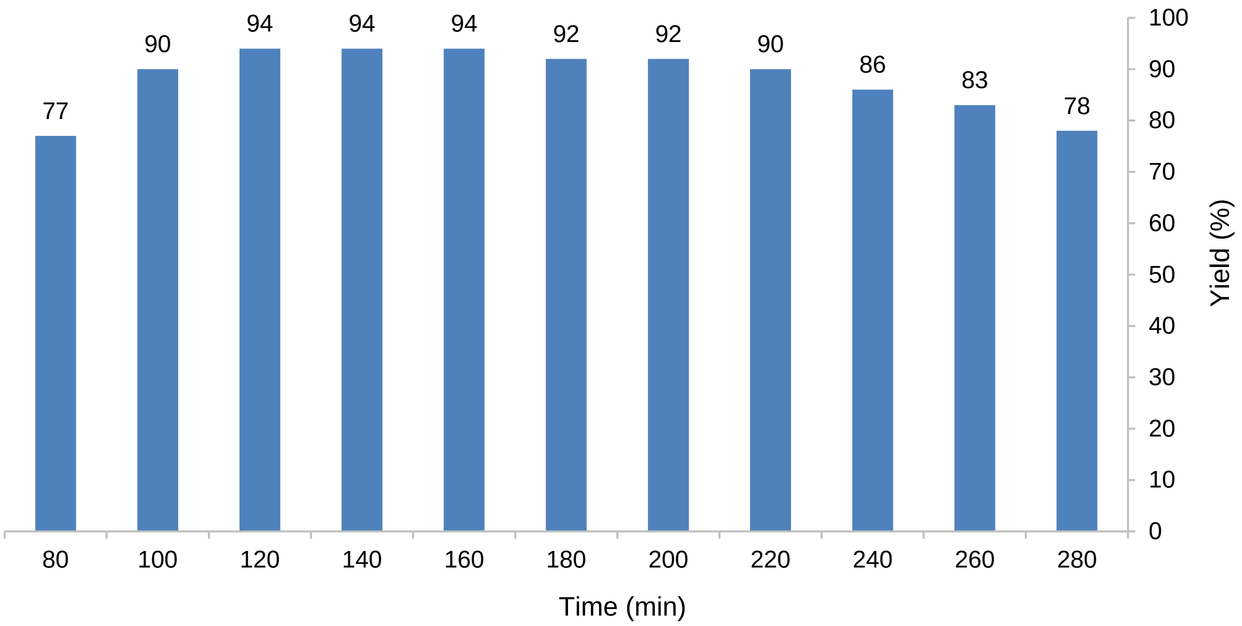

Fig. S15. HPLC yield profile of the tetracaine precursor samples collected over the run time.

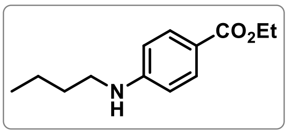

Ethyl 4-(butylamino)benzoate (3b). Prepared according to the isolation run procedure **C2**. The product **3b** was obtained as white solid (1.49 g, 84% yield). The characterization of the compound matches the data reported in the literature.[S5]

D. Optimization of the reaction conditions

D1. Optimization of the reaction conditions for the model reaction

A series of optimization experiments were performed using ethyl 4-bromobenzoate (**1**) and pyrrolidine (**2a**) as model reagents in order to explore the reaction parameters. These experiments were carried out following General Procedure **C1**. Yields were determinate by calibrated HPLC analysis using 4-ethylbiphenyl as the internal standard:

$$[\boldsymbol{3a}] = \left(\frac{Area\ (\boldsymbol{3a})}{Area\ (IS)} - c\right) \times \frac{[IS]}{k}$$

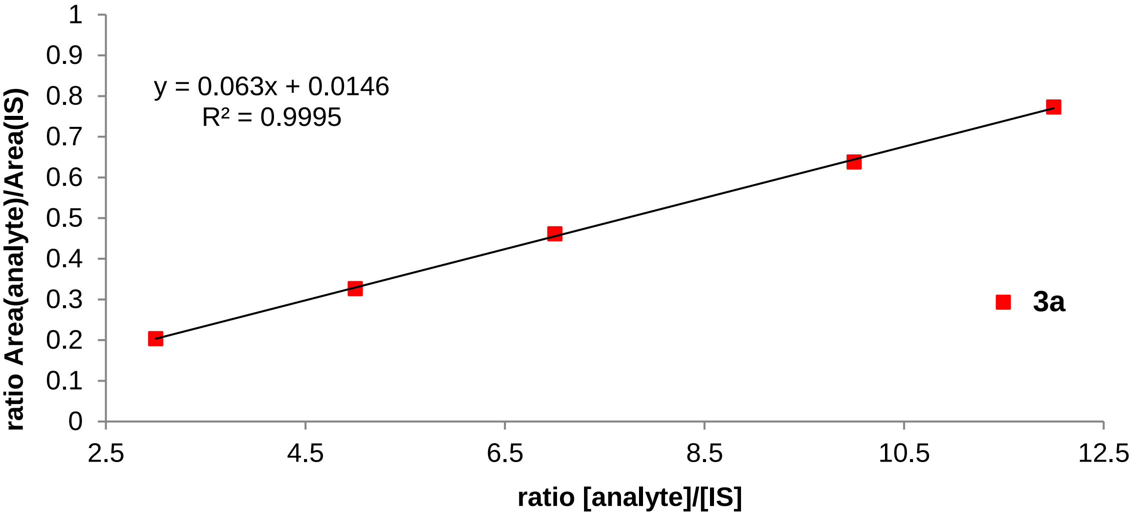

Fig. S16. HPLC calibration curve for the model reaction.

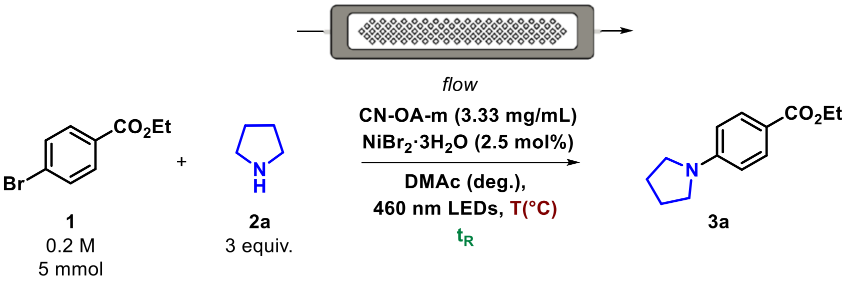

Table S3. Screening of the reaction parameters (residence time, temperature and pulsation amplitude and frequency). Reactions were performed on 5 mmol scale, 25 mL stock solution. [a]Yields were determined by HPLC using 4-ethylbiphenyl as the internal standard at the concentration maximum. [b]50% LED power.

Entry	Residence Time	Temperature	Pulsation Amplitude	Pulsation Frequency	Yield[a]
1	15 min	40°C	70%	100%	66%
2	15 min	50°C	70%	100%	77%
3	15 min	50°C	30%	100%	83%
4	15 min	50°C	20%	100%	86%
5	20 min	50°C	20%	100%	94%
6	20 min	50°C	20%	50%	99%
7	20 min	50°C	20%	50%	89%[b]

In order to test the reproducibility of these results, an experiment was conducted 3 times, using the conditions from Table S3 entry 3 (83% max yield). The yield/concentration vs time curves are shown below (Fig. S17) and as can be seen, no significant difference in yield is observed once higher concentrations are reached.

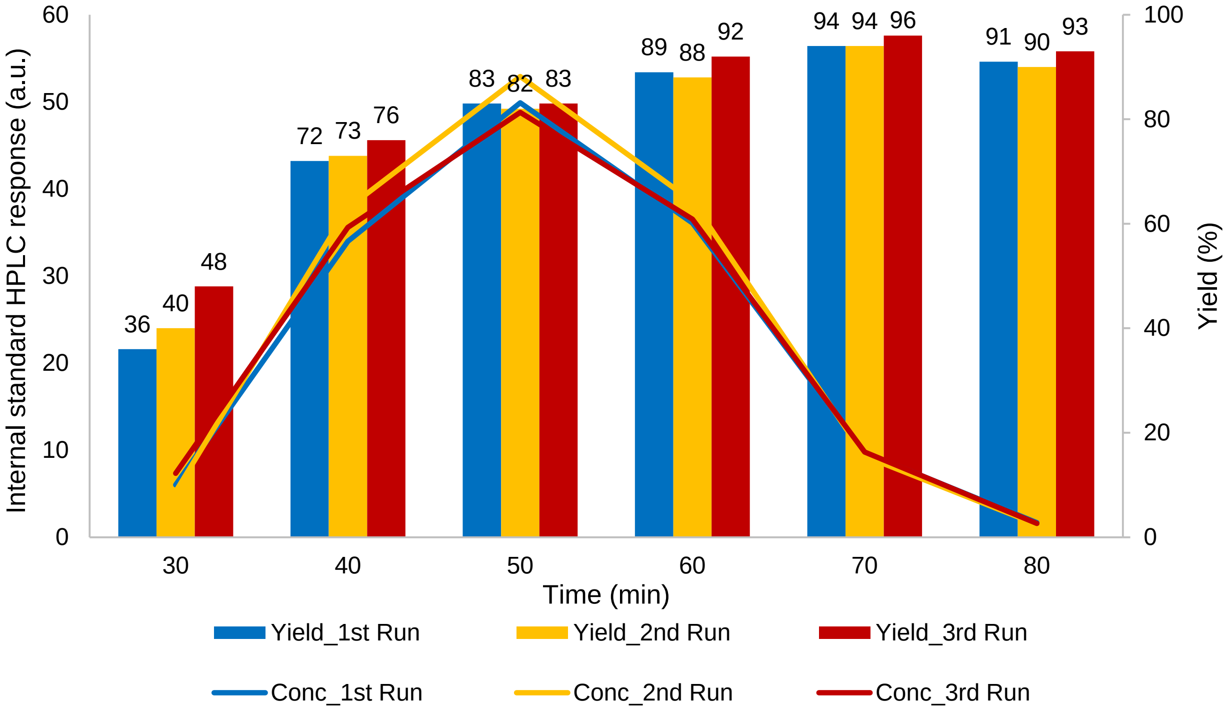

Fig. S17. Three repetitions of experimental conditions from Table S3, entry 3, to confirm reproducibility. Reaction conditions: 15 min residence time, 50 °C, 30% amplitude, 100% frequency. Yields and concentrations were determined by HPLC using 4-ethylbiphenyl as the internal standard.

A series of experiments were performed to optimize the pulsation amplitude in order to find a suitable match between an appropriate carbon nitride dispersion and the minimum longitudinal diffusion (back mixing). For the physical correlation between the numerical values of the pulsation amplitude and the displaced volume see Section B3.

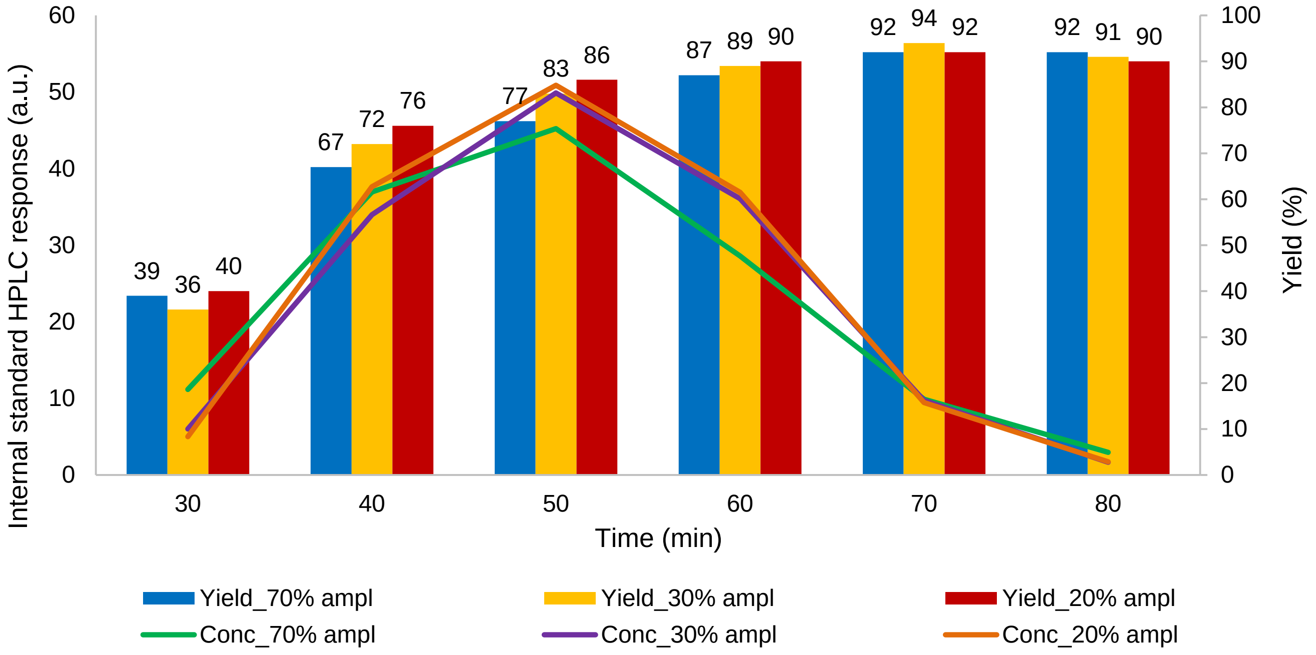

Fig. S18. Effect of the pulsation amplitude. Reaction conditions: 15 min residence time, 50°C. Yields and concentrations were determined by HPLC using 4-ethylbiphenyl as the internal standard.

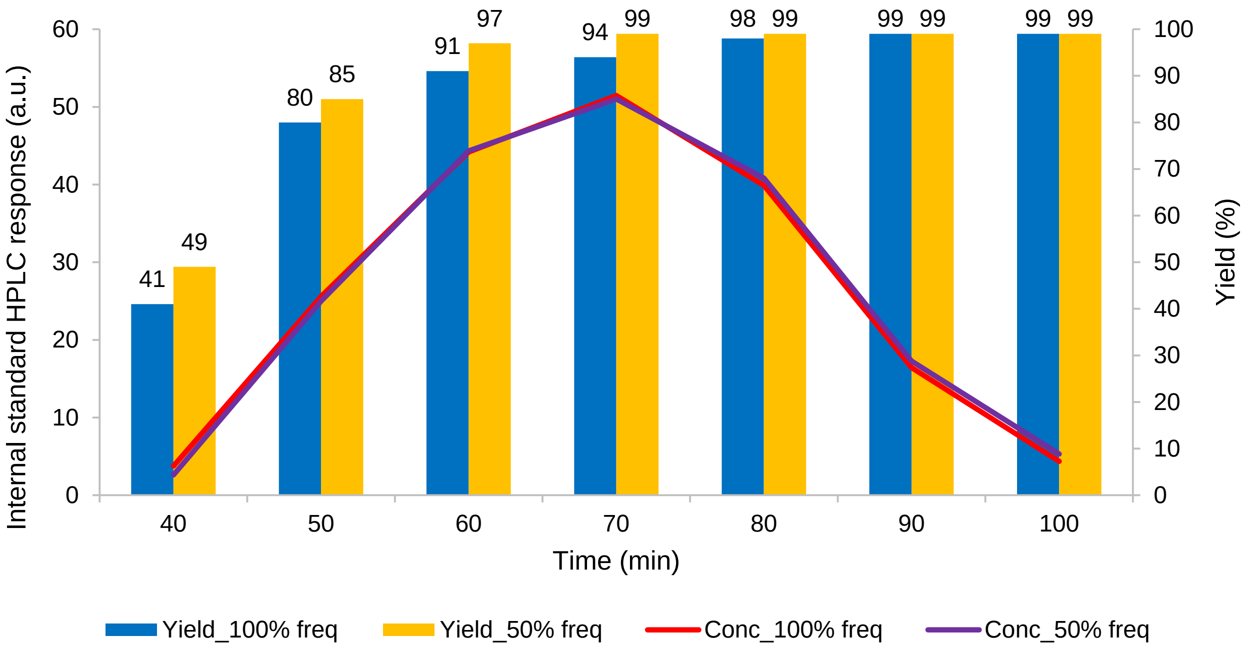

Fig. S19. Effect of the pulsation frequency. Reaction conditions: 20 min residence time, 50°C. Yields and concentrations were determined by HPLC using 4-ethylbiphenyl as the internal standard.

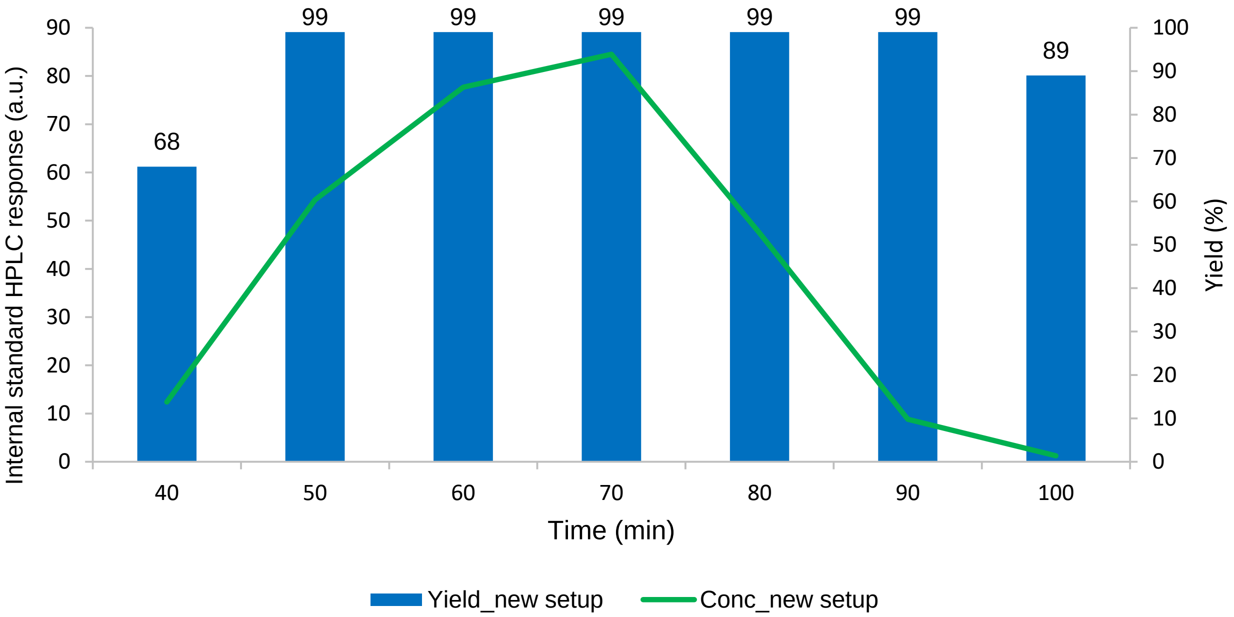

Fig. S20. Concentration/yield profile of the reaction performed in the new setup at 0.3 M. Reaction conditions: 20 min residence time, 50°C. Yields and concentrations were determined by HPLC using 4-ethylbiphenyl as the internal standard.

D2. Optimization of the reaction conditions for the tetracaine precursor synthesis

A series of optimization studies were performed using ethyl 4-bromobenzoate (**1**) and butylamine (**2b**) as reagents to prepare the tetracaine precursor (**3b**) at 20% pulsation amplitude and 50% pulsation frequency. These experiments were carried out following General Procedure **C2**. Yields were determinate by calibrated HPLC analysis using 4-ethylbiphenyl as the internal standard.

$$[\boldsymbol{3b}] = \left(\frac{Area\ (\boldsymbol{3b})}{Area\ (IS)} - c\right) \times \frac{[IS]}{k}$$

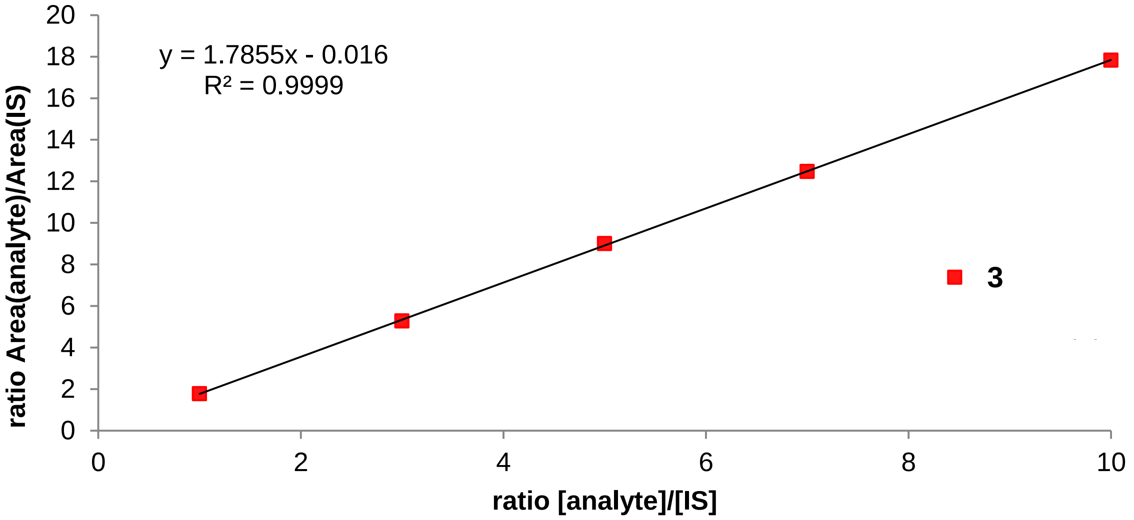

Fig. S21. HPLC calibration curve for the tetracaine precursor.

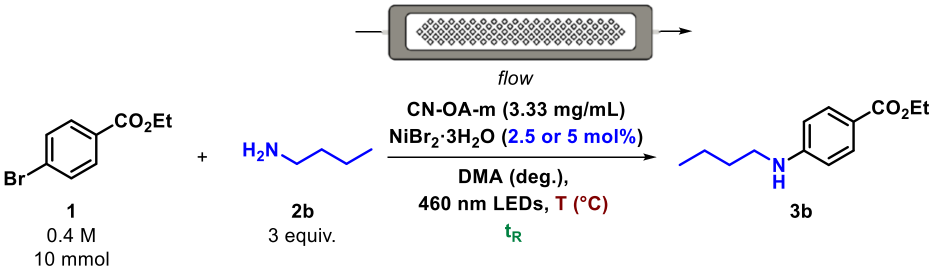

Table S4. Screening of the reaction parameters (residence time, temperature, concentration, Ni loading) for the tetracaine precursor synthesis. Reactions were performed on 5 to 10 mmol scale, 25 mL stock solution at 20% pulsation amplitude and 50% pulsation frequency. CN-OA-m loading was kept the same for all the experiments carried out. [a]Yields were determined by HPLC using 4-ethylbiphenyl as the internal standard at the concentration maximum.

Entry	Residence Time	Temperature	Concentration	$NiBr_2 \cdot 3H_2O$	Yield[a]
1	20 min	60°C	0.2 M	2.5 mol%	24%
2	20 min	60°C	0.3 M	2.5 mol%	30%
3	20 min	60°C	0.4 M	5 mol%	38%
4	60 min	60°C	0.4 M	5 mol%	69%
5	60 min	73°C	0.4 M	5 mol%	85%
6	60 min	80°C	0.4 M	5 mol%	94%

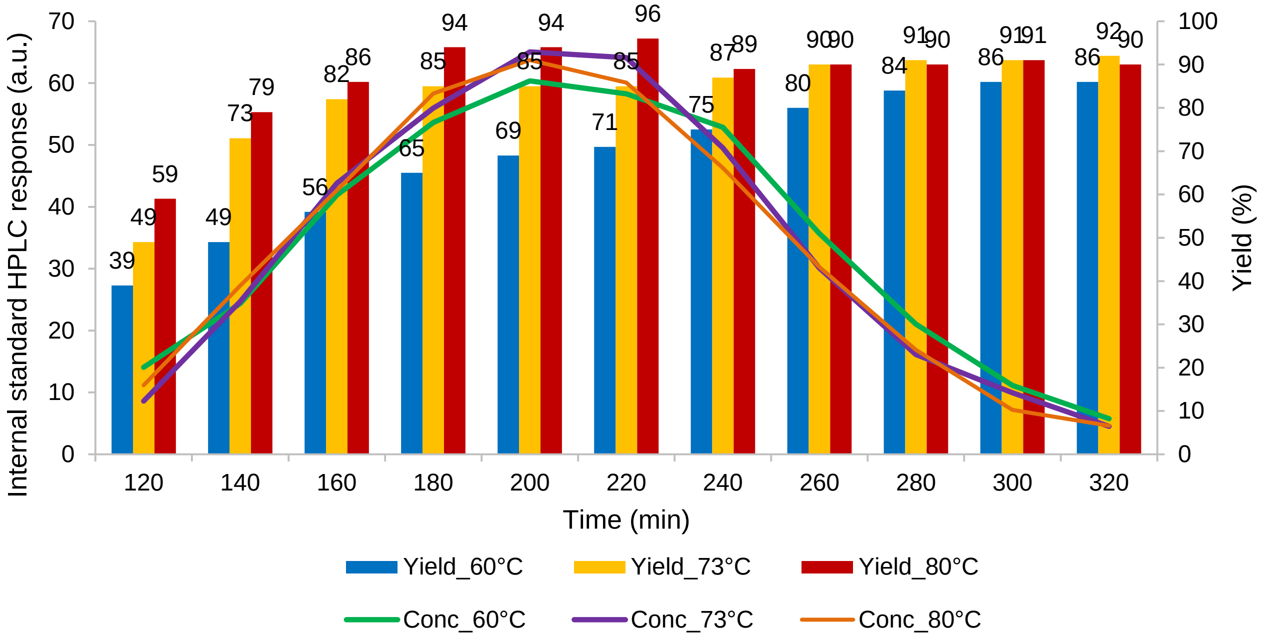

Fig. S22. Effect of the temperature. Reaction conditions: 60 min residence time, 5 mol% $NiBr_2 \cdot 3H_2O$, 0.4 M. Yields and concentrations were determined by HPLC using 4-ethylbiphenyl as the internal standard.

E. Particle size distribution (PSD) of CN-OA-m

In order to determine the particle size distribution (PSD) of the CN-OA-m, a series of Laser Diffraction (LD) measurements were carried out. Preliminarily, a mixture of CN-OA-m in DMAc (3.33 mg/mL) was pumped through the reaction system (screening experiments setup, Fig. S1) at 0.75 mL/min, 20% pulsation amplitude and 50% pulsation frequency to simulate a reaction. Therefore, the particles that can pass through the apparatus can be separated from those which in the tubing after the reactor. The latter ones were finally removed by flushing the system at 10 mL/min flow rate and maximum pulsation. The two materials were individually collected, analyzed by LD using the parameters defined in section **A1** and compared with the unprocessed CN-OA-m. The resulting PSD profiles are shown in Fig. S23.

The D10, D50 and D90 values for these particles were recorded:

D10 = Diameter at which 10% of particles are smaller.

D50 = Median particle diameter.

D90 = Diameter at which 90% of particles are smaller.

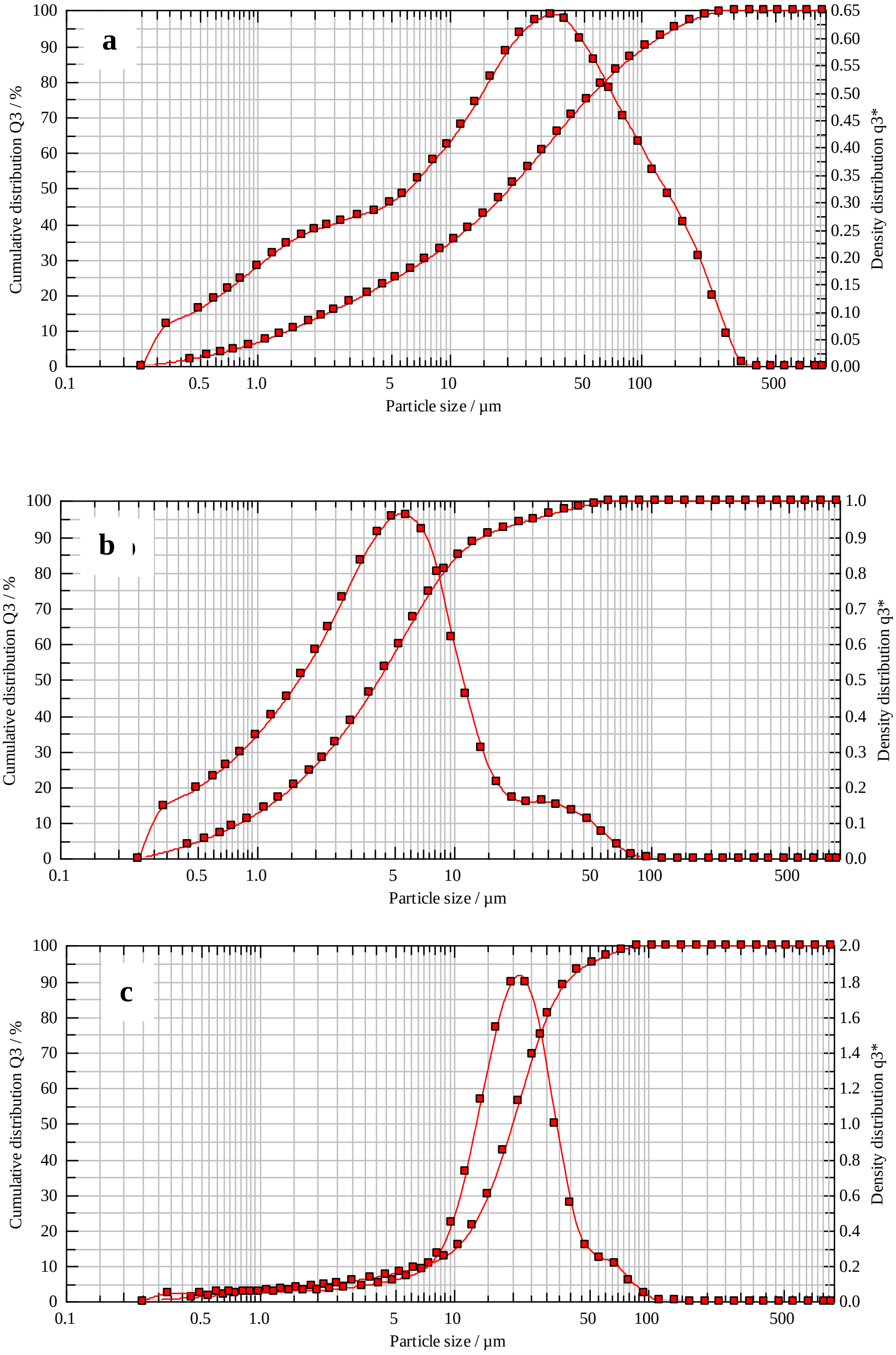

Fig. S23. PSD profiles obtained from LD analysis. a) unprocessed CN-OA-m; b) particles passed through the reactor system; c) particles which stuck in the tubing after the reactor.

The particles passed through the system have shown a PSD centered on ≈ 5 µm (D10 = 0.9 µm, D50 = 4.3 µm, D90 = 15 µm, Fig. S23b). On the other hand, particles which stuck in the tubing have shown a PSD centered on ≈ 20 µm (D10 = 7 µm, D50= 20 µm, D90 = 40 µm, Fig. S23c). Both the distributions are present in the unprocessed CN-OA-m PSD (Fig. S23a).

Ball milling of the material was attempted (Retsch MM 400 mill) in efforts to reach a single size distribution, but this failed to show any change from the original PSD (Fig. S23a).

F. References

S1 B. Pieber, J. A. Malik, C. Cavedon, S. Gisbertz, A. Savateev, D. Cruz, T. Heil, G. Zhang and P. H. Seeberger, *Angew. Chem. Int. Ed.*, 2019, **58**, 9575–9580.

S2 O. Levenspiel, *Chemical Reaction Engineering*, John Wiley & Sons, 3rd edn., 1999.

S3 A. Pomberger, Y. Mo, K. Y. Nandiwale, V. L. Schultz, R. Duvadie, R. I. Robinson, E. I. Altinoglu and K. F. Jensen, *Org. Process Res. Dev.*, 2019, **23**, 2699–2706.

S4 I. Ghosh, J. Khamrai, A. Savateev, N. Shlapakov, M. Antonietti and B. König, *Science,* 2019, **365**, 360–366.

S5 A. E. Wahba and M. T. Hamann, *J. Org. Chem.*, 2012, **77**, 4578–4585.

G. NMR spectra

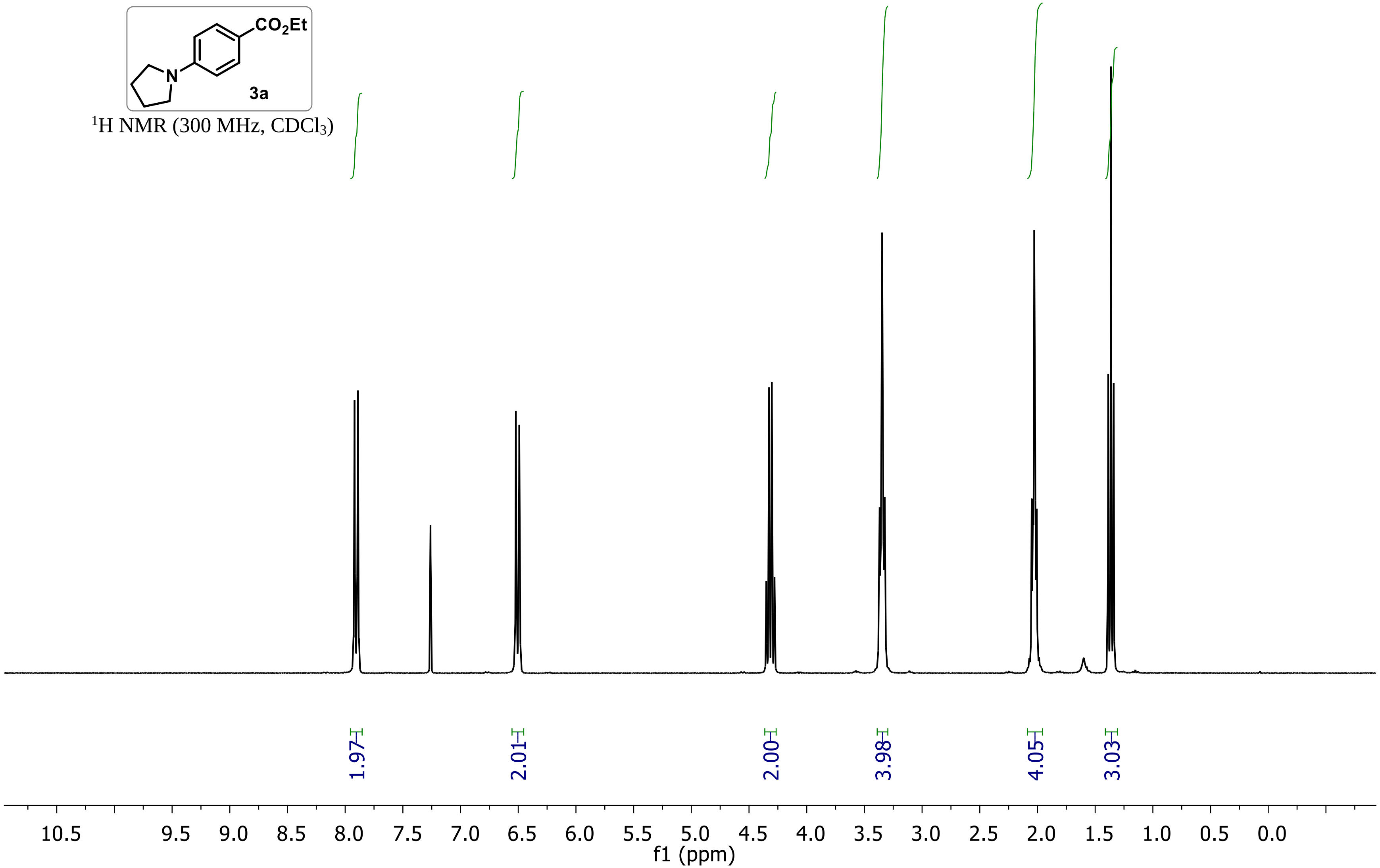
3a

^{1}H NMR (300 MHz, $CDCl_3$)

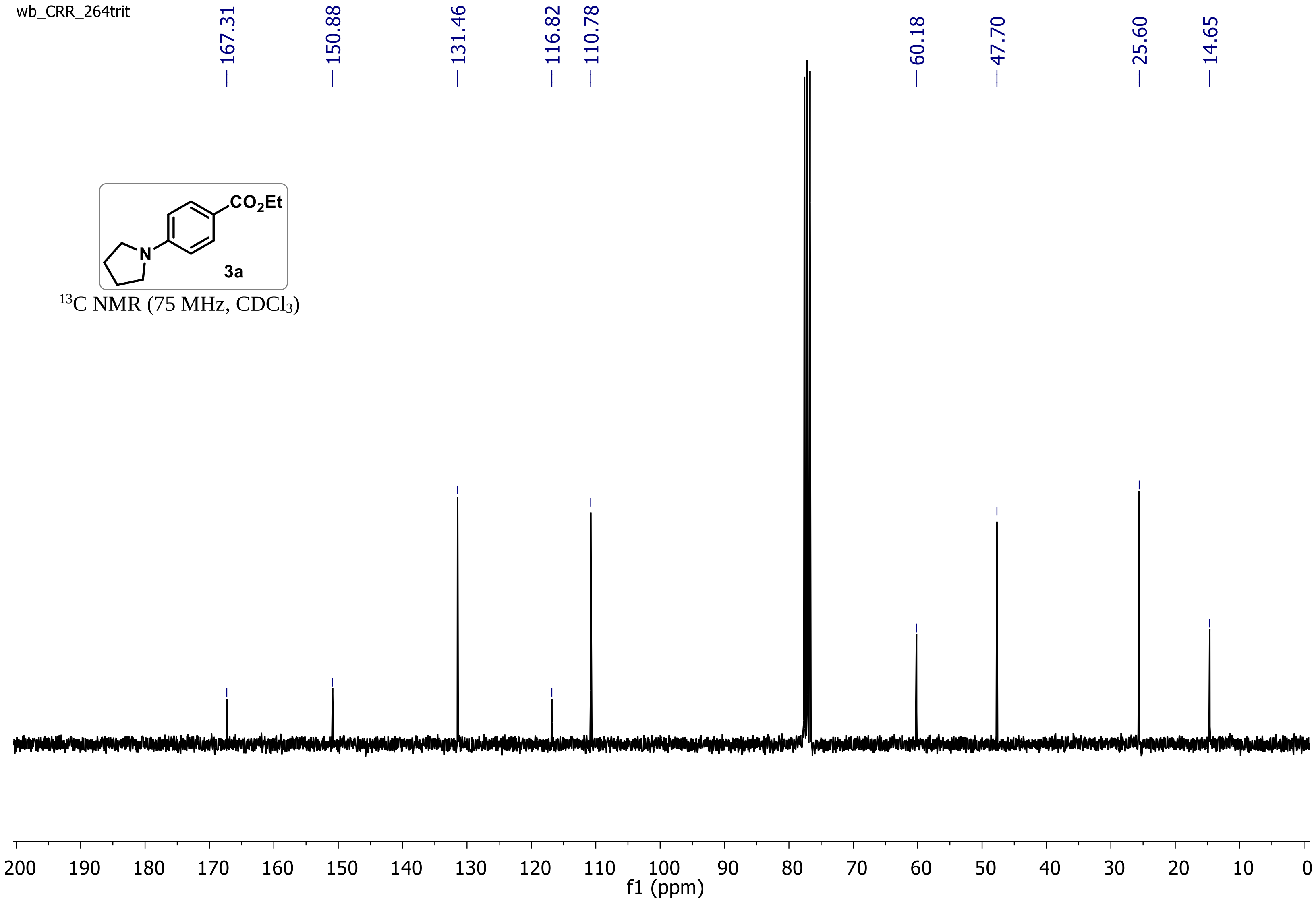

3a

^{13}C NMR (75 MHz, $CDCl_3$)

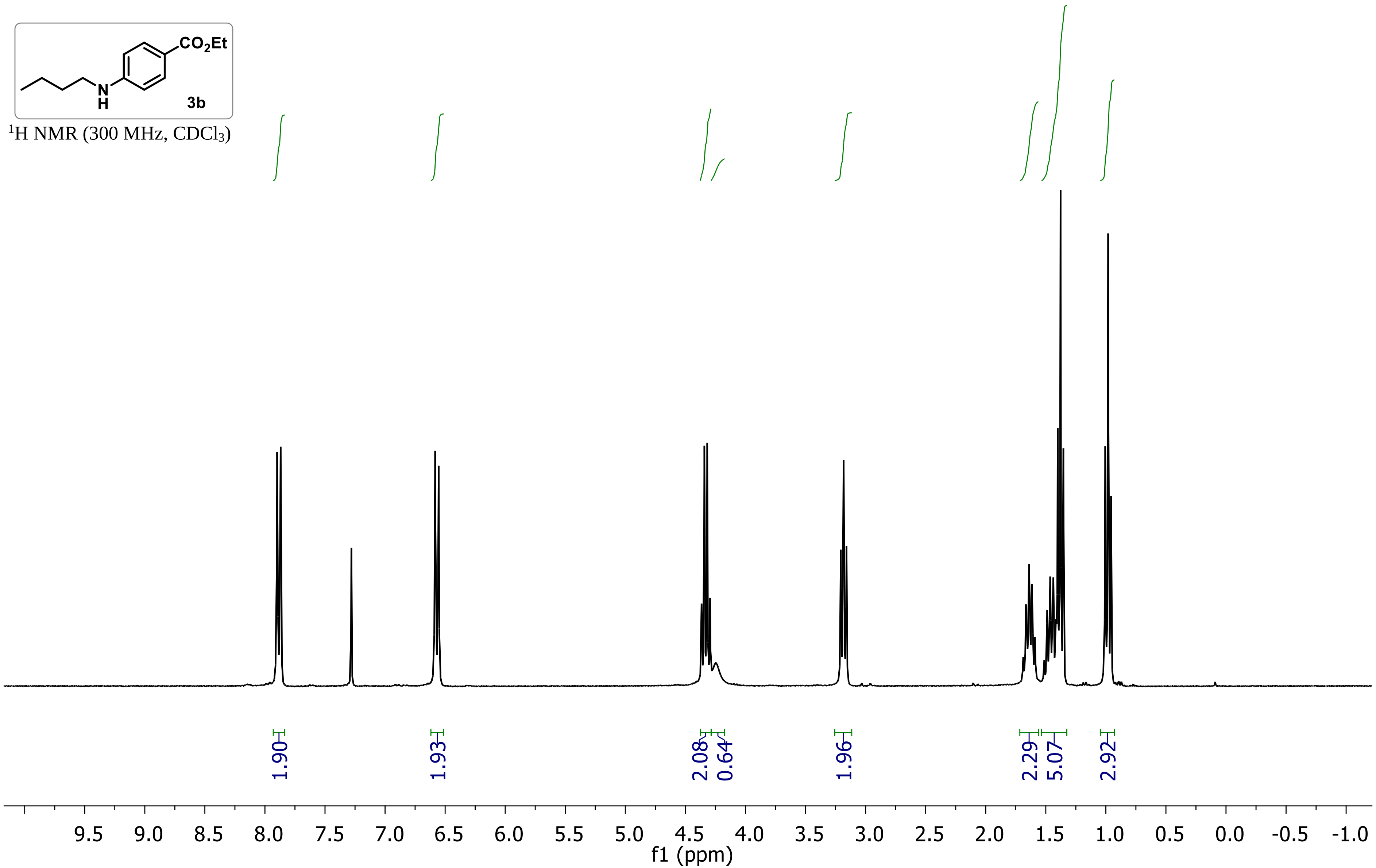

3b

^{1}H NMR (300 MHz, CDCl$_3$)

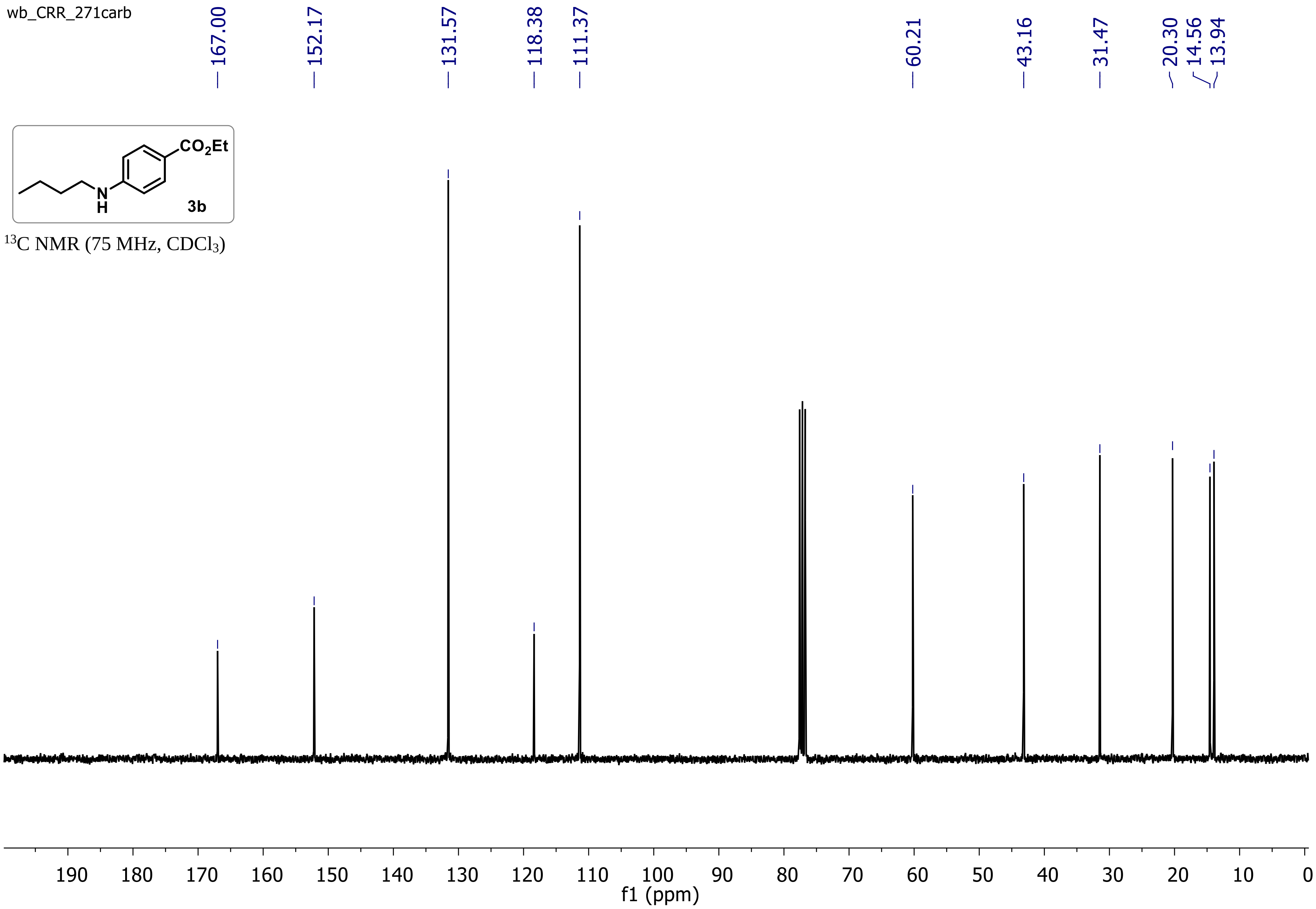

^{13}C NMR (75 MHz, $CDCl_3$)